Electronic structure and magnetic properties of pyroxenes $(Li,Na)TM(Si,Ge)_2O_6$: Low-dimensional magnets with 90° bonds

S. V. Streltsov[1,2,*] and D. I. Khomskii[3]
[1]*Institute of Metal Physics, S. Kovalevskoy St. 18, 620041 Ekaterinburg GSP-170, Russia*
[2]*Ural State Technical University, Mira St. 19, 620002 Ekaterinburg, Russia*
[3]*II. Physikalisches Institut, Universität zu Köln, Zülpicher Straße 77, D-50937 Köln, Germany*
(Received 16 October 2007; published 4 February 2008)

The results of the LSDA+U calculations for pyroxenes with diverse magnetic properties $(Li,Na)TM(Si,Ge)_2O_6$, where TM is the transition metal ion (Ti, V, Cr, Mn, Fe), are presented. We show that the anisotropic orbital ordering results in the spin-gap formation in $NaTiSi_2O_6$. The detailed analysis of different contributions to the intrachain exchange interactions for pyroxenes is performed both analytically using perturbation theory and basing on the results of the band structure calculations. The antiferromagnetic $t_{2g}-t_{2g}$ exchange is found to decrease gradually in going from Ti to Fe. It turns out to be nearly compensated by ferromagnetic interaction between half-filled t_{2g} and empty e_g orbitals in Cr-based pyroxenes. The fine tuning of the interaction parameters by the crystal structure results in the ferromagnetism for $NaCrGe_2O_6$. Further increase of the total number of electrons and occupation of e_g subshell makes the $t_{2g}-e_g$ contribution and total exchange interaction antiferromagnetic for Mn- and Fe-based pyroxenes. Strong oxygen polarization was found in Fe-based pyroxenes. It is shown that this effect leads to a considerable reduction of antiferromagnetic intrachain exchange. The obtained results may serve as a basis for the analysis of diverse magnetic properties of pyroxenes, including those with recently discovered multiferroic behavior.

DOI: 10.1103/PhysRevB.77.064405 PACS number(s): 71.20.−b, 74.25.Ha, 72.80.Ga

I. INTRODUCTION

Pyroxenes with the general formula AMX_2O_6 are an extremely rich class of compounds. Here, A may be alkali Na, Li, or alkaline-earth Ca, Sr, etc., elements, M different metals with the valence 3+, X is most typically Si^{4+}, but also Ge^{4+}, and could even be V^{5+}. These systems are best known in geology and mineralogy: they are one of the main rock-forming minerals in the Earth's crust and are also found on the Moon, planets, and in meteorites. One of the pyroxenes, $NaCrSi_2O_6$, may be found in natural form only in meteorites, which is reflected in its name: mineral kosmochlore. Another one, $NaAlSi_2O_6$, is the famous Chinese jade. For the condensed matter physics, the pyroxenes with M a transition metal (TM) are of particular interest because of their rich and interesting magnetic properties.

Structurally magnetic subsystem in pyroxenes is quasi-one-dimensional: TMO_6 octahedra form edge-sharing zigzag chains connected by the chains of XO_4 tetrahedra (see Fig. 1). Two aspects are here especially important. First of all, the edge-sharing character with TM–O–TM angle close, but not exactly equals to 90°, which results in the competition between different contributions to the superexchange (see Sec. II). Second, a "shifted" packing of neighboring TM chains leads to the situation, when every TM ion is connected (via own O and XO_4 tetrahedra) with two TM ions in neighboring chain. Thus, the general topology of exchange interaction is triangularlike [see Fig. 2(a)], and the magnetic system may be frustrated.

Both these factors may lead to nontrivial magnetic properties of pyroxenes, which are indeed observed experimentally, although for most of them the detailed studies are still absent. There are among them antiferromagnetic [e.g., $(Li,Na)V(Si,Ge)_2O_6$ (Ref. 4) $(Li,Na)Fe(Si,Ge)_2O_6$ (Ref. 5)] and even ferromagnetic [e.g., $NaCrGe_2O_6$ (Ref. 6)] insulators. Some of the pyroxenes have the ground state with the spin gap: $CaCuGe_2O_6$ (Ref. 7) and $NaTiSi_2O_6$,[8,9] although the nature of such a state is apparently different: this seems to be due to formation of interchain dimers in $CaCuGe_2O_6$ (Ref. 10) and due to the intrachain dimerization in $NaTiSi_2O_6$, stabilized by the special type of orbital order.[8,9,11]

Finally, a new twist in this story is the recent discovery that the pyroxenes apparently form a new class of multiferroics.[1] It was found that at least three of them, $NaFeSi_2O_6$, $LiFeSi_2O_6$, and $LiCrSi_2O_6$, develop an electric

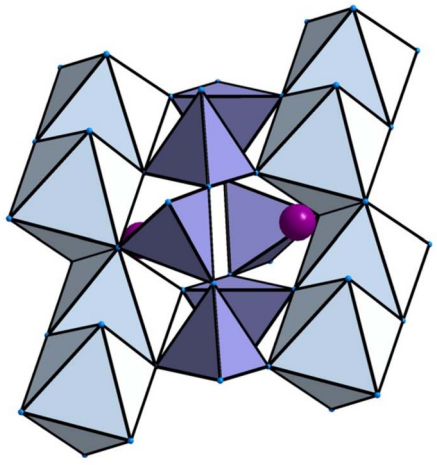

FIG. 1. (Color online) Crystal structure of pyroxenes. Two chains made of TMO_6 octahedra and its connections via XO_4 (where X is usually Si or Ge) tetrahedra are shown. Purple balls represent Li(Na) ions.

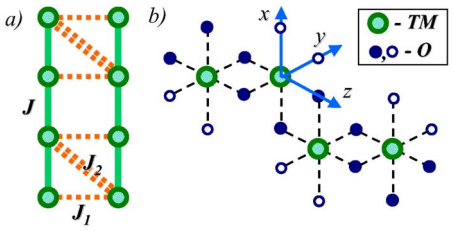

FIG. 2. (Color online) (a) Triangularlike topology of the TM network in pyroxenes. Solid lines are intrachain links and dashed and double-dashed lines are the interchain connection via one or two XO_4 tetrahedra; J, J_1, and J_2 are the corresponding exchange parameters. (b) Sketch of the one of TMO_6 chains. Two different types oxygens are shown. Those depicted as solid circles belongs to two different TMO_6 octahedra and open circle only to one. The later oxygens are called "side oxygens" in the text. The natural choice of the local coordinate system, when z axis is directed along the single 180° O–TM–O bond connecting two neighboring TMO_6 octahedra, is shown.

polarization in a magnetically ordered state, below ~6 K in $NaFeSi_2O_6$, ~18 K in $LiFeSi_2O_6$, and ~11 K in $LiFeSi_2O_6$. Similar to other multiferroics with magnetically driven ferroelectricity (see, e.g., reviews[2,3]), electric polarization in them can be strongly modified by a magnetic field. Note also that the most pyroxenes are insulating (often beautifully colored crystals), which makes them especially good for studying eventual ferroelectricity.

To understand magnetic properties of this large and important class of compounds, and especially to have a better understanding of the possible mechanism of multiferroic behavior in them, it is desirable to know the details of the exchange coupling. The knowledge of orbital occupancy is also very important, both in connection with their structure and for determining the details of exchange interactions. To reach this goal and also to provide better understanding of an electronic structure of pyroxenes in general, we undertook a detailed theoretical investigation of these problems, concentrating on systems with A=Na,Li, X=Si,Ge, and different trivalent TM ions. We carried out detailed *ab initio* calculations and, in particular, obtained the values of the exchange constants. Besides these values themselves, which can be useful for interpreting the properties of real materials, we paid main attention to the study of the systematics of the exchange in different compounds of this large class, and to particular mechanisms, or partial contributions of different exchange passes to the total exchange. General conclusions reached are important for the analysis of the multiferroic behavior in pyroxenes, they may be useful also for understanding of the properties of pyroxenes with alkaline-earth A ions such as, e.g., $CaMnSi_2O_6$, and may serve as a very good illustration of different tendencies in exchange couplings in systems with complicated geometry in general.

II. DIFFERENT CONTRIBUTIONS TO EXCHANGE

Before presenting the results of our *ab initio* calculations, let us first discuss the different mechanisms of the intrachain exchange interaction. The explicit expressions for it may be calculated using the perturbation theory in t/U_{dd} or t/Δ, where t is an effective electron hopping (either direct d-d hopping t_{dd} or hopping between d states of TM and $2p$ states of oxygen t_{pd}), U_{dd} is an on-site Coulomb interaction, and Δ is a charge-transfer energy (energy of the promotion of an electron from $2p$ states of oxygen to $3d$ states of TM).

The main motive of the intrachain packing of TM ions in pyroxenes is the edge-sharing packing of TMO_6 octahedra (see Fig. 1), with 90° TM–O–TM bonds for (half)filled $t_{2g}-t_{2g}$ and $t_{2g}-e_g$ orbitals. This implies that one of the important contributions will be a direct exchange between partially filled t_{2g} orbitals, the lobes of which look toward the neighboring TM ions. This contribution to the total exchange will be antiferromagnetic (AFM) and proportional to

$$J_{t_{2g}-t_{2g}} \sim \frac{t^2_{t_{2g}-t_{2g}}}{U_{dd}}, \tag{1}$$

where $t_{t_{2g}-t_{2g}}$ is the $t_{2g}-t_{2g}$ hopping parameter due to direct overlap of d-wave functions. Since consecutive TM–O–TM planes in zigzag TM chains are rotated by 90° [see Fig. 2(b)], specific orbital pattern will be crucial for this contribution. This, in particular, leads to strongly alternating exchange in $NaTiSi_2O_6$, determining the appearance of the spin gap in it (see Sec. IV). On the other hand, the corresponding orbital occupation in V pyroxenes does not lead to an alternating exchange (Sec. V). Of course, for t^3_{2g} occupation, as for Cr^{3+} or Fe^{3+}, all the pairs between neighboring TM ions belonging to the same chain would have equal contributions to this part of the exchange.

Due to the decrease of the radius of d orbitals and, with it, of $t_{2g}-t_{2g}$ hopping, this direct exchange is expected to strongly diminish in going from Ti to Fe pyroxenes (see below). Note that we use the terminology "direct exchange" for the exchange caused by the direct d-d overlap and hopping, and reserve the term "superexchange" for the exchange mediated by oxygens.[12]

Besides direct d-d hopping, p-d hybridization leads to an important contribution to the total exchange due to TM–O–TM hopping. Different possible situations leading to a superexchange via oxygens are illustrated in Figs. 3–5. In these figures the (half) occupied orbitals of TM are shown as filled (blue or hatched red) and empty orbitals as empty (white) ones. From these figures, it is clear that the corresponding contributions can be both antiferromagnetic and ferromagnetic.

The simplest case is that of Fig. 3(a). Here, the half-filled orbitals at neighboring TM's overlap with the same oxygen p orbital. According to the usual rules,[13] this antiferro-orbital ordering gives a substantial AFM exchange,

$$J^{SE}_{t_{2g}-t_{2g}} \sim \frac{t^4_{pd\pi}}{\Delta^2}\left(\frac{1}{2\Delta+U_{pp}}+\frac{1}{U_{dd}}\right). \tag{2}$$

Here, $t_{pd\pi}$ is the π hopping between t_{2g} and $2p$ orbitals. It is important that the magnitude of t_{2g}-O-t_{2g} (e_g-O-e_g) exchange presented in Eq. (2) does not strongly depend on the TM–O–TM angle α (only via dependence of t_{pd} hopping on α). First and second contributions are due to the correlation and

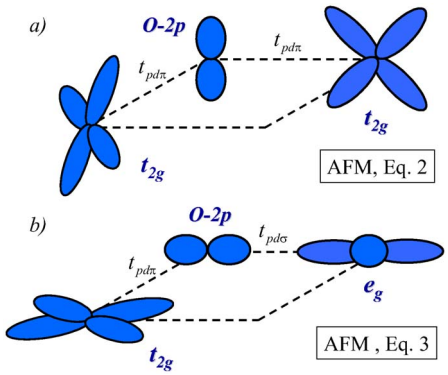

FIG. 3. (Color online) Typical orbital ordering between two occupied TM d orbitals via the same O $2p$ orbital, which results to AFM interaction for the case of 90° TM–O–TM bond.

delocalization effects in terminology of Ref. 13.

Similarly, in the case of Fig. 3(b), half-filled t_{2g} and e_g orbitals overlap via the same oxygen orbital, which gives even stronger AFM exchange,

$$J^{SE}_{t_{2g}-e_g} \sim \frac{t^2_{pd\pi} t^2_{pd\sigma}}{\Delta^2}\left(\frac{1}{2\Delta + U_{pp}} + \frac{1}{U_{dd}}\right), \tag{3}$$

where $t_{pd\sigma}$ is the hopping between e_g orbital of TM and $2p$ orbital of oxygen directed toward it. $t_{pd\sigma}$ is approximately two times larger than $t_{pd\pi}$.[14]

If the hopping is only possible from the occupied to an empty d orbital, or if occupied orbitals of TM do not overlap with the same oxygen orbital, the resulting contribution to the exchange turns out to be ferromagnetic.

First of all, let us consider the situation when one of d orbitals is empty and it overlaps with the same oxygen p orbitals, as the occupied d orbital [see Figs. 4(a) and 4(b)]. Then, electrons can virtually hop to this empty orbital, but Hund's rule coupling J^{TM}_H tends to orient spins at an ion parallel. This will result in a ferromagnetic (FM) exchange,

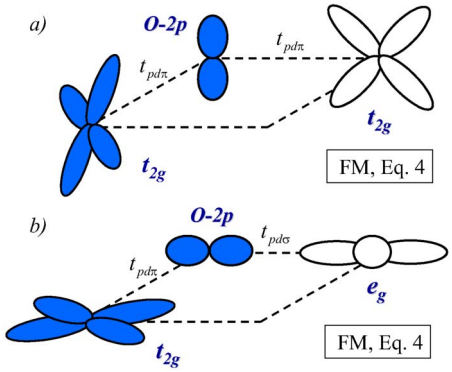

FIG. 4. (Color online) Typical orbital ordering between occupied (filled) and unoccupied (unfilled) d orbitals of TM via the same O $2p$ orbital, which results to FM interaction for the case of 90°TM–O–TM bond.

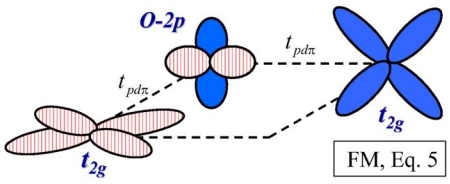

FIG. 5. (Color online) Typical orbital ordering between two occupied d orbitals of TM via *different* O $2p$ orbitals, which results in a FM interaction for the case of 90° TM–O–TM bond.

$$J^{SE}_{t_{2g}-t_{2g}/e_g} \sim -\frac{t^2_{pdm} t^2_{pdm'}}{\Delta^2}\left(\frac{J^{TM}_H}{(2\Delta + U_{pp})^2} + \frac{J^{TM}_H}{U^2_{dd}}\right). \tag{4}$$

Note that J^{TM}_H here is Hund's energy gain when we put an extra electron with parallel spin to the original state of a TM ion, i.e., depending on the total spin of the latter, J^{TM}_H may be equal, e.g., to twice the usual atomic value of $J_H \sim 0.8$ eV for $3d$ series when the spin of the TM ion is $S=1$ (two electrons with parallel spins as in V^{3+}), or $3J_H$, as for Cr^{3+} (d^3, $S=3/2$). This may enhance the ferromagnetic contribution in certain cases (in particular, for Cr systems).

The last contribution to the total d-d exchange interaction is coming from the overlap of occupied d orbitals with different (orthogonal) $2p$ orbitals. Typical orbital pattern for this situation is shown in Fig. 5, but one may draw similar pictures also for the case of e_g/e_g or e_g/t_{2g} orbitals. This exchange will be FM again because of Hund's rule, but in this case acting in oxygen $2p$ shell. With such an overlap, the consecutive hopping of the electrons from one d ion to another one through oxygen p shell (delocalization exchange of Ref. 13) turns out to be forbidden. Two oxygen's electrons are hopping to different TM ions instead. Because of Hund's coupling on oxygen (J^p_H), the FM ordering becomes more favorable,

$$J^{SE}_{t_{2g}/e_g-t_{2g}/e_g} \sim -\frac{t^2_{pdm} t^2_{pdm'} J^p_H}{\Delta^2(2\Delta + U_{pp})^2}, \tag{5}$$

Note that t_{pdm} in expressions (4) and (5) may be $t_{pd\pi}$ or $t_{pd\sigma}$, depending on the particular case. For instance, for the case depicted in Fig. 4(b), one of them is $t_{pd\pi}$ and another is $t_{pd\sigma}$.

In order to describe the magnetic interactions in a particular pyroxene, one has to include in general all possible contributions discussed above, via both common oxygens, and take into account several general trends.

First of all, the radius of d states (r_d) and with them the direct d-d (t_{dd}) hoppings decrease going from the light to heavy TM (from Ti, V to Fe). According to the famous Harrison scaling,[14]

$$t_{dd} \sim \frac{r^3_d}{D^5}, \tag{6}$$

where D is the distance between TM. Taking into account typical values for r_d presented in Ref. 14 and assuming that D is the same, we found that $t^{\mathrm{Ti}}_{dd} \sim 2.5 t^{\mathrm{Fe}}_{dd}$. Thus, only this effect may provide suppression of the direct exchange in Fe-based pyroxenes comparing with those based on Ti by a

factor of 6. Second, the distance between TM ions D by itself strongly affects the exchange coupling, as seen from Eq. (6). Third, there exist the strong increase of U_{dd} and decrease of the charge-transfer energy Δ for the late TM's. Δ enters expressions (2)–(5) in the denominators either as Δ^2 or even as Δ^4 and plays very important role. For Ti^{3+}, Δ equals to 6 eV, whereas for Fe^{3+}, it is 2.5 eV only.[15] This factor leads for the late $3d$ elements to an increase of the role of superexchange via oxygen, which competes with the direct d-d exchange dominating in early TM's.

The qualitative discussion presented in this section will serve as a framework for interpreting the results of the following sections. As we will see, all these factors are quite important and indeed determine the tendencies of exchange constants in pyroxenes and many other systems with 90° TM–O–TM bonds.

III. COMPUTATIONAL DETAILS

Crystallographic data used in the calculations were taken from the following papers: $NaTiSi_2O_6$ (T=100 K, space group P-1),[16] $LiVSi_2O_6$ (T=293 K, space group $C2/c$),[17] $NaVSi_2O_6$ (T=296 K, space group $C2/c$),[18] $LiCrSi_2O_6$ (T=100 K, space group $P2_1/c$),[19] $NaCrSi_2O_6$ (T=300 K, space group $C2/c$),[20] $NaCrGe_2O_6$ (T=293 K, space group $C2/c$),[21] $NaMnSi_2O_6$ (T=302 K, space group $C2/c$),[22] $NaFeSi_2O_6$ (T=14 K, space group $C2/c$),[23] and $LiFeSi_2O_6$ (T=100 K, space group $P2_1/c$).[5]

There is a controversy in the literature about the crystal structure of $NaVGe_2O_6$ and $LiVGe_2O_6$. Although all the studies were performed for the room temperature, the difference in lattice parameters exceeds 0.3 Å for $NaVGe_2O_6$.[4,24] There is also uncertainty about the space group for this material.[24,25] In contrast to $NaVGe_2O_6$, there is no striking disagreement about the crystal structure of $LiVGe_2O_6$ in Refs. 4 and 24. However, we were not able to reproduce distances presented in Ref. 24 from their crystal structure. Therefore, the study of electronic and magnetic properties of both $NaVGe_2O_6$ and $LiVGe_2O_6$ was postponed for the future, when all the problems about the crystal structure of these compounds would be resolved.

The primary calculations were performed within the framework of the linear muffin-tin orbital method (LMTO).[27] The values of on-site Coulomb interaction (U) and Hund's rule coupling (J_H) parameters were taken as follows: U_{Ti} =3.3 eV, U_V=3.5 eV, U_{Cr}=3.7 eV, and $U_{Mn,Fe}$=4.5 eV; J_H =0.8 eV for Ti, V, and Cr, J_H=0.9 eV for Mn, and J_H =1 eV for Fe. The values of U and J_H for Ti were calculated for the same Ti radii in Ref. 26. For other TM, those parameters were taken as an average in wide variety of values of U and J_H for TM^{3+} ions presented in the literature. For the material with small values of exchange parameters (cromates), we checked that the small variation of U ($\pm$0.5 eV) does not change magnetic ground state.

Instead of LSDA+U approximation used in Ref. 9, we utilized LSDA+U approach in the present paper. The difference between these two methods is in the parts of the Hamiltonian allowed to be spin polarized. In the LDA+U method, only d shell of the transition metal ions may be spin polarized; for all the other ions, different spin states are averaged out. This allows more easy account of the double counting in LDA+U formalism, but does not treat correctly the effects of possible spin polarization of oxygens, which significantly restricts the applicability of the method to more complex systems. We found the noticeable spin polarization of oxygens for the late TM pyroxenes (Mn and Fe, see Sec. VII) in the LSDA+U calculations and used this approach for the whole series. For the Ti and V systems, the effects of oxygen polarization is insignificant and these two approximations give essentially the same results. For Fe-based pyroxenes, LDA +U overestimated exchange constants by as much as $\sim$25%–30%.

The second difference from the Ref. 9 is the more careful choice of the MT radii. We found that for not uniform atom distribution in dimerized $NaTiSi_2O_6$, the LMTO calculation is very sensitive to the radii of Na MT sphere. As a result of too large R_{Na}=3.5 a.u. used in Ref. 9, Na ion takes the electrons in excess, which leads to the significant overestimate of the exchange constant. In the present paper, we used R_{Na} =3.3 a.u. for all pyroxenes. This choice of R_{Na} results in good agreement with the band structure and exchange constants obtained in the pseudopotential calculations, as it will be discussed in Sec. IV. Note, however, that the main conclusions about the importance of the strong Coulomb correlations made in Ref. 9 are valid and do not depend on the choice of R_{Na}. In addition, it is interesting enough that only the results for $NaTiSi_2O_6$ significantly depend on R_{Na}. Other pyroxenes do not show such a strong dependence. For instance, by going from R_{Na}=3.5 a.u. to R_{Na}=3.3 a.u. for $NaCrGe_2O_6$, the exchange constants change by 1.1 K, and for $NaCrSi_2O_6$, even less, 0.2 K.

The radii of other elements were set as follows: R_O =1.65–1.75 a.u., $R_{Si,Ge}$=1.9 a.u., and R_{Li}=2.9 a.u. The radii of transition metals were chosen to be R_{TM}=2.4–2.67 a.u.

The Ti,V,Cr,Mn,Fe($4s,4p,3d$), O($2s,2p,3d$), Si($3s,3p,3d$), Ge($4s,4p,4d$), Li($2s,2p,3d$), and Na($3s,3p,3d$) orbitals were included to the orbital basis set in our calculations. The Brillouin-zone (BZ) integration in the course of the self-consistency iterations was performed over a mesh of 64 **k** points in the irreducible part of the BZ. For those systems for which exchange parameters are particularly small, the calculation was checked by the finer mesh of 216 **k** points.

In our notations, Heisenberg Hamiltonian is written in the following form:

$$H = \sum_{ij} J_{ij} \vec{S}_i \vec{S}_j, \tag{7}$$

where summation runs twice over every pair i,j. J were computed in the framework of Lichtenstein's exchange interaction parameter (LEIP) calculation procedure.[28] According to the LEIP formalism, exchange constants J can be calculated as the second derivatives of the energy variation at small spin rotation. For s=1/2,

$$J_{ij} = \frac{\mathrm{Im}}{\pi} \int_{-\infty}^{E_F} d\epsilon \sum_{\substack{mm' \\ m''m'''}} \Delta_i^{mm'} G_{ij\downarrow}^{m'm''} \Delta_j^{m''m'''} G_{ji\uparrow}^{m'''m}, \qquad (8)$$

where m, m', m'', and m''' are the magnetic quantum numbers, i,j the lattice indexes, $\Delta_i^{mm'} = H_{ii\uparrow}^{mm'} - H_{ii\downarrow}^{mm'}$ is the on-site potential correction due to different spins, and the Green's function is calculated in the following way:

$$G_{ij\sigma}^{mm'}(\epsilon) = \sum_{k,n} \frac{c_{i\sigma}^{mn}(k) c_{j\sigma}^{m'n*}(k)}{\epsilon - E_\sigma^n}. \qquad (9)$$

Here, σ is the spin index, $c_{i\sigma}^{mn}$ is a component of the nth eigenstate, and E_σ^n is the corresponding eigenvalue. Since transition metal ions are usually magnetic, the Green's functions $G_{ij\sigma}^{mm'}(\epsilon)$ and potential corrections $\Delta_i^{mm'}$ are computed only for them.

The great advantage of the LEIP procedure is the possibility to calculate not only total J's between corresponding sublattices of transition metal ions, but, since it is linear with respect to the magnetic quantum numbers, one can also compute partial contributions, which come from different d orbitals.

These orbitals were defined in the local coordination system (LCS), where axes are orthogonal and directed as much as possible to the neighboring oxygens. The natural choice of the LCS is when the local z axis is directed along the only 180° O–TM–O connecting two neighboring TMO_6 octahedra [see Fig. 2(b)]. This definition is unique, and it is used for all the pyroxenes studied in the present paper.

Since some of the exchange constants obtained within the LMTO method using LEIP were found to be sensitive to the choice of MT radii, in the present paper, we rechecked the LMTO results by calculating the exchange constants from the total energies in the pseudopotential PW-SCF code.[29] The formalism of pseudopotential method does not require the introduction of any atomic spheres. We used ultrasoft pseudopotentials with nonlinear core correction taken from www.pwscf.org with different forms of exchange-correlation functional. The plane-wave and kinetic energy cutoffs were chosen to be 40 and 200 Ry, respectively. 216 k points were used in the course of self-consistency.

Hopping integrals were obtained using Wannier function projection in LMTO method described elsewhere.[26,30] Small subspace defined by three t_{2g} orbitals (defined in LCS) per V atom was used in this procedure. Since for all of the considered pyroxenes t_{2g} bands are well isolated, the resulting projected and initial LDA bands completely coincide.

IV. Ti-BASED PYROXENE: $NaTiSi_2O_6$ (d^1)

As it was discussed in detail in Sec. I, pyroxenes are made of isolated zigzag chains of TMO_6 octahedra. Combination of low dimensionality together with the small value of the spin moment in $NaTiSi_2O_6$ results in an opening of the spin gap.[8,31] Here, we will show that it becomes possible due to a particular orbital ordering.

Two different models were suggested in order to explain the physical origin of the spin-gap formation. The first one (dimer model) was initially proposed in experimental papers[8,32] and supported afterward by the LDA+U calculations.[9] It takes into account quite strong dimerization of Ti-Ti chain found in very detailed structural study performed by Redhammer *et al.*[16] According to this model, the ground state of $NaTiSi_2O_6$ consists of spin singlet Ti-Ti dimers, and the spin-gap observed in the experiment is the energy gap between spin singlet and triplet states of these dimers.

In another model (Haldane scenario)[34,35] Ti-Ti dimers were proposed to be in a spin triplet state and such $S=1$ Ti-Ti pairs form the AFM chain, which is known as Haldane chain[33] with the spin gap $\Delta_{SG}=0.41J$, where J is the exchange constant.

Thus, the key point in these two scenarios is the degeneracy of the magnetic ground state of Ti-Ti dimer: in the dimers model, it is a singlet, but in the Haldane one, a triplet.

It is interesting to note that depending on the situation the pair of metal ions may have quite different degeneracy of the magnetic ground state. In the case of isolated cluster of metal atoms in vacuum, the ions in the pair are very tightly bound and must be considered as one quantum-mechanical object. The bond length of such isolated "metal-metal molecule," respectively, is quite small: 1.9 Å for Ti-Ti pair.[36] The spin configuration in this case will be governed by Hund's coupling, which favors the state with larger multiplicity. As a result, the ground state of isolated metal-metal dimers usually is *not* the singlet one.[36]

However, the situation in insulating transition metal oxides is qualitatively different. Typical metal-metal distance varies here depending on the type of the crystal structure, but usually it is much larger than in isolated dimers: Ti-Ti distance is 3.1 Å in the edge-sharing octahedral structure of $NaTiSi_2O_6$.[16] As a result, every ion has its own ground state configuration, and the influence of the other ions can be incorporated via perturbation theory.[13] The resulting electronic Hamiltonian can be reduced to a Heisenberg model,[37] which is known to have spin-singlet ground state for the dimer. Our band-structure calculations in LSDA+U approximation give the same result: rather strong antiferromagnetic exchange in short Ti-Ti dimers $J_{intra}=396$ K, and the weak exchange between dimers $J_{inter}=5$ K.

The electronic structure of $NaTiSi_2O_6$, obtained in the LSDA+U approach is presented in Fig. 6. Both the top of the valence band and bottom of conduction one are formed by Ti $3d$ states, divided by the band gap of 1.77 eV. Singly occupied Ti $3d$ orbital has zy character. The Corresponding ferro-orbital ordering is shown in Fig. 7. In a short Ti-Ti pair, it results in a strong direct exchange interaction, which is AFM in agreement with Goodenough-Kanamori-Anderson rules.[13,37] On the other hand, for the long Ti-Ti pairs the orbitals are directed in such a way that the overlap between them is almost zero, which leads to a rather small interdimer exchange.

Note that the exchange constants presented above are different from those given in Ref. 9. This is due to a more careful choice of Na MT radii, as it was discussed in Sec. III. In the present paper, we additionally checked the LMTO results by calculating total energies using pseudopotential PW-SCF code.[29] In order to have reliable result, the calcula-

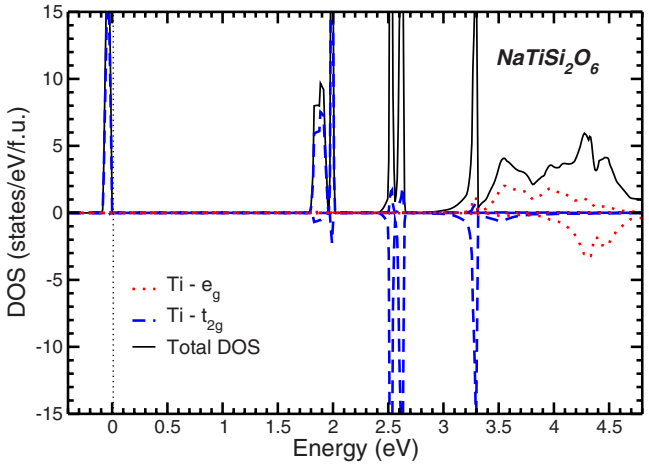

FIG. 6. (Color online) Total and projected DOS for $NaTiSi_2O_6$ obtained in LSDA+U calculation. Total DOS is the sum for both spins. Up (down) panel corresponds to spin majority (minority). Fermi level is zero energy.

tions with the use of two different pseudopotentials based on Perdew-Wang-91 (PW91) and Perdew-Bruke-Ernzerhof (PBE) exchange potentials were utilized. The total energy difference between FM and AFM solutions were found to be 398 K for PW91 and 395 K for PBE, which are very closed to the present LMTO results.

One should be careful comparing exchange constants obtained in the band-structure calculation with the value of the spin gap. This is due to strong quantum effects. What is indeed calculated by any mean-field method are the total energies for AFM and FM configurations (or the change of these energies with respect to the small rotation angle of spins, as in LEIP, which is essentially the same). For the case of isolated dimer $s=1/2$ and Heisenberg model defined by Eq. (7), the total energy difference between FM and AFM configurations equals to J. The spin gap Δ_{SG} is the energy difference between *quantum* singlet and triplet states, which are not the same as collinear AFM and FM states. For $s=1/2$, the spin gap $\Delta_{SG}=2J$. The spin gap obtained for $NaTiSi_2O_6$ using different experimental methods is about 600–700 K.[31] This agrees with $\Delta_{SG}\sim 790$ K calculated in the presented paper.

V. V-BASED PYROXENES (d^2)

Ionic configuration of V in the pyroxenes is d^2 implying $S=1$. Because of a larger spin moment, it is much harder to make dimerized chains in V-based pyroxenes. The spin gap may still appear in the system, if it could be considered as a set of isolated one-dimensional AFM chains of $S=1$ (Haldane chains[33]). However, experimentally, all the V pyroxenes show long-range magnetic ordering at low temperatures.[4] Three different reasons for it were discussed in the literature: biquadratic exchange,[38,39] interchain exchange,[40,41] and next-nearest-neighbor coupling.[38]

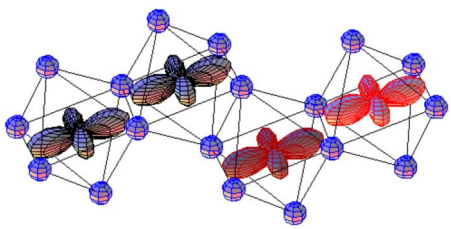

FIG. 7. (Color online) The orbital ordering obtained in LSDA+U calculations for $NaTiSi_2O_6$ is shown.

TABLE I. Results of the LSDA+U calculations for different pyroxenes. The values of the band gap and spin moments were taken from AFM (intrachain) solution intrachain calculations for all the compounds, except $NaCrGe_2O_6$. The exchange parameters were obtained in LEIP formalism.

	Ionic conf. of TM	Band gap (eV)	Spin mom. (μ_B)	Exchange intrachain (K)
$NaTiSi_2O_6$	d^1	1.77	0.92	396
$LiVSi_2O_6$	d^2	1.92	1.87	50.3
$NaVSi_2O_6$	d^2	1.80	1.85	15.0
$LiCrSi_2O_6$	d^3	3.57	2.78	3.4
$NaCrSi_2O_6$	d^3	3.03	2.83	−0.8
$NaCrGe_2O_6$	d^3	2.88	2.84	−5.2
$NaMnSi_2O_6$	d^4	1.76	3.69	3.4
$LiFeSi_2O_6$	d^5	1.63	4.02	15.8[a]
$NaFeSi_2O_6$	d^5	2.31	4.24	15.9[a]

[a]Note that because of the large O $2p$ polarization, the exchange parameters obtained in LEIP formalism are significantly overestimated for Fe-based pyroxenes (see Sec. VIII).

Common structural feature for all of the pyroxenes except Mn-based ones (they are Jahn-Teller active) is the presence of two short TM–O bonds. These are the bonds with "side oxygens," see Fig. 2(b).

Short V-O bonds form nearly 90° angle. Such a distortion of TMO_6 octahedra may be represented as two independent compressions in the x and y directions. As a result, zx and zy orbitals will be almost degenerate and have lower energy than xy.

In our LSDA+U calculations two $3d$ electrons of V follow the crystal-field splitting and occupy the zx and zy orbitals, i.e., these systems do not have orbital degeneracy. Each orbital provides strong AFM direct exchange with one of the neighboring V. This leads, as we will show below, to the uniform exchange interaction in each chain, with the direct exchange defined in Eq. (1). The superexchange via oxygens would be also homogeneous and (weaker) FM.

In our calculations, all the $(Li,Na)VSi_2O_6$ pyroxenes were found to be insulators with the band gap of 1.8–1.9 eV. Spin moments are slightly reduced from ionic value of $2\mu_B$ because of the hybridization. Interestingly, the calculated intrachain exchange constants significantly decrease going from Li↦Na (see Table I). In order to understand the reasons for such tendency, we took advantage of the LEIP and calculated partial contributions to the total exchange constants.

We found that as in $NaTiSi_2O_2$, in V pyroxenes, the most important contribution is the direct exchange interaction between t_{2g} orbitals. For $LiVSi_2O_2$ $J_{t_{2g}-t_{2g}}=59.6$ K. The $t_{2g}-e_g$ partial exchange is FM since it occurs from occupied to empty orbital. Numerically, this contribution is defined by Eq. (4), and in our LSDA+U calculation for $LiVSi_2O_2$ $J_{t_{2g}-e_g}=-9.9$ K. The rest, 0.6 K (total exchange for $LiVSi_2O_2$ is 50.3 K), is the partial exchange between e_g orbitals, which should be completely empty in the purely ionic picture, but which still are partially occupied in the real band structure calculation because of the hybridization with oxygens.

Going from Li to Na, the $t_{2g}-t_{2g}$ partial exchange weakens because of the increase of the distances and local distortions of the octahedra. For $NaVSi_2O_2$, $J_{t_{2g}-t_{2g}}=27.5$ K, $J_{t_{2g}-e_g}=-13.3$ K, and $J_{e_g-e_g}=0.8$ K. The direct calculation of hopping integrals corroborates this interpretation. Thus, e.g., for $LiVSi_2O_6$ and $NaVSi_2O_6$, the ratio of $t_{2g}-t_{2g}$ exchange integrals $J^{\mathrm{Li}}_{t_{2g}}/J^{\mathrm{Na}}_{t_{2g}}=2.17$, which is close to the squared ratio between effective $t_{2g}-t_{2g}$ hopping integrals $(t^{\mathrm{Li}}/t^{\mathrm{Na}})^2=2.15$.

The total values of intrachain interaction obtained within LMTO method $J=50.3$ K ($LiVSi_2O_6$) and $J=15.0$ K ($NaVSi_2O_6$) agree with those calculated in pseudopotential code from the total energies: $J=51.3$ K ($LiVSi_2O_6$) and $J=13.8$ K ($NaVSi_2O_6$). In addition, it matches the exchange constants obtained in Ref. 40, where the fitting of experimental curves of magnetic susceptibility to theoretical one, obtained using quantum Monte Carlo simulations on a cubic lattice, was performed. Note, however, that Pedrini *et al.*[40] used different definitions of Heisenberg Hamiltonian, and their exchanges must be divided by factor two to compare with ours. In addition, it should be mentioned that the real geometry of pyroxenes includes frustrating diagonal exchange paths depicted in Fig. 2(a) as dashed lines. Those contributions were not taken into account in Ref. 40.

VI. Cr-BASED PYROXENES (d^3)

Generally, the electronic properties of Cr-based (d^3 configuration, $S=3/2$) pyroxenes are similar to those of other pyroxenes: they are also insulators, but with larger band gap of ~3 eV. This is mainly because of the fact that spin-majority t_{2g} subshell becomes fully occupied and goes lower in energy. More important is that the character of the valence band in Cr-based pyroxenes is different.

Both the Ti- and V-based pyroxenes were found to be Mott-Hubbard insulators, with the gap separating occupied and unoccupied transition metal 3d bands. Going from the left to the right in the same row of the Periodic Table, the charge-transfer energy decreases, O 2p states shift up,[15] and get to the same energy region as the lower transition metal Hubbard band. This is clearly seen from the DOS plot obtained for $NaCrSi_2O_6$ in LSDA+U calculation and presented in Fig. 8. Quite similar situation occurs in other Cr-based transition metal oxides: one may observe significant mixing between O 2p and Cr 3d states at the top of the valence band.[42,43] This feature of the electronic structure is important for the magnetism of Cr-based pyroxenes since it increases superexchange interaction via O 2p states.

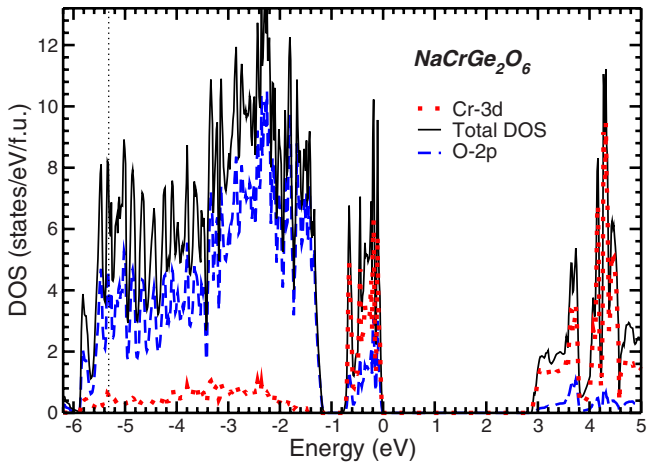

FIG. 8. (Color online) Total and projected DOS for $NaCrGe_2O_6$ obtained in LDA+U calculation. Fermi level is zero energy.

Experimentally, $LiCrSi_2O_6$ and $NaCrSi_2O_6$ were found to be AFM with small Néel temperatures, 11 and 3 K, respectively; $NaCrGe_2O_6$ is FM with $T_C=6$ K.

In our calculations, $LiCrSi_2O_6$ was indeed found to be AFM with $J=3.4$ K. $NaCrSi_2O_6$ shows rather small intrachain exchange, less than 1 K. This number is obviously lying beyond the precision of the calculation scheme.[44] One may just note that this compound is on the borderline between FM and AFM orderings. In agreement with the experiment, intrachain exchange in $NaCrGe_2O_6$ is FM and more pronounced, $J=-5.2$ K (−7.9 K in pseudopotential calculation).

More detailed investigation of the partial contributions to intrachain exchange shows that $t_{2g}-e_g$ exchange interaction in all Cr-based pyroxenes is almost the same as in V-based ones: $J^{SE}_{t_{2g}-e_g}\sim-10.5$ K. The AFM $t_{2g}-t_{2g}$ contribution, in contrast, is significantly reduced in Cr pyroxenes. This seems to be the joint effect of the increase of the TM-TM distances and on-site Coulomb repulsion U and the decrease of the charge-transfer energy Δ and radii of localization of d electron r_d, as it was discussed in the end of Sec. II.

The largest $t_{2g}-t_{2g}$ exchange was found in $LiCrSi_2O_6$: $J_{t_{2g}-t_{2g}}=13.4$ K, which has shortest Cr-Cr distance ($D=3.06$ Å). For $NaCrSi_2O_6$, the $t_{2g}-t_{2g}$ exchange is smaller, $J_{t_{2g}-t_{2g}}=7.7$ K, which is presumably related to longer Cr-Cr distance ($D=3.086$ Å). Thus, according to our calculations, the FM $t_{2g}-e_g$ exchange almost compensates AFM $t_{2g}-t_{2g}$ contribution in $NaCrSi_2O_6$. This tendency continues for $NaCrGe_2O_6$, where because of larger Ge and Na ionic radii the Cr-Cr distance exceeds its maximum value ($D=3.142$ Å), and the FM $t_{2g}-e_g$ contribution becomes dominating since $J_{t_{2g}-t_{2g}}=3.1$ K.

Changes of the electronic structure going from Si to Ge on the example of Cr-based pyroxenes

The Cr-based pyroxenes were the only pyroxenes with available and reliable crystal structure to study the effect of Si↔Ge interchange in these compounds. We studied only these, but argue that the general character of the changes in

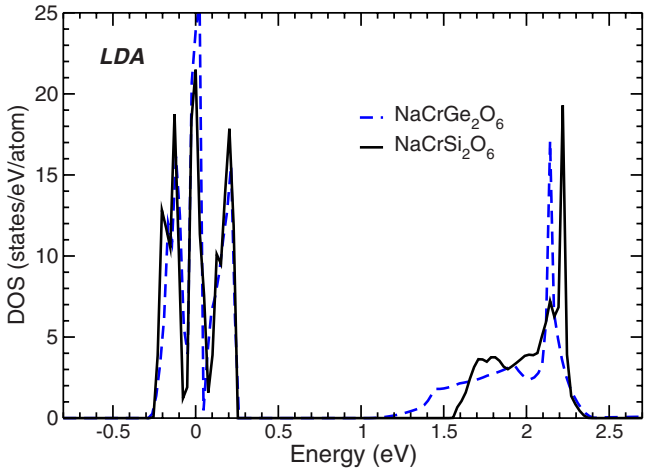

FIG. 9. (Color online) Cr $3d$ DOS for $NaCrSi_2O_6$ and $NaCrGe_2O_6$ obtained in LDA. It illustrates the decrease of the $t_{2g}-e_g$ crystal-field splitting with substitution Si by Ge. Fermi level is zero energy.

the electronic structure should be the same for other pyroxenes.

There are two possible mechanism, which may determine the difference in the electronic properties of Ge and Si based pyroxenes. First of all, Ge $4p$ states have larger spatial extensions than Si $3p$, this may result in larger covalency effects. Second, the size of Ge^{4+} ions is much larger than Si^{4+} (the ionic radius $R^{IV}_{Ge^{4+}}=0.39$ Å, while $R^{IV}_{Si^4}=0.24$ Å). Therefore, different structural distortions are expected for Ge and Si pyroxenes.

In order to understand how important is the effect of $4p$ or $3p$ states, we performed the calculations, where in the $NaCrGe_2O_6$, Ge ions were substituted by Si. In this case, all the distances in "artificial $NaCrSi_2O_6$" were taken the same as in the parent $NaCrGe_2O_6$. All the radii of MT spheres were also taken the same as for $NaCrGe_2O_6$. The results show minor difference in shape and positions of Cr d bands compared to $NaCrGe_2O_6$. Therefore, one may conclude that the origin of the difference in the electronic properties between Si and Ge pyroxenes is mostly due to different local distortions.

The average Ge-O bond distance ($d_{Ge\text{-}O}=1.74$ Å in $NaCrGe_2O_6$) is larger than Si-O one ($d_{Si\text{-}O}=1.63$ Å in $NaCrSi_2O_6$). Since the TM-O distance is mostly determined by the strong ionic TM-O bond and hence by the TM and O ionic radii only, the substitution of Si by larger Ge leads to the bending of TM–O–TM bond. If in $NaCrSi_2O_6$ the angle Cr-O-Cr=99.6°, then in $NaCrGe_2O_6$, this angle is 101.2°. This leads to an increase of the Cr e_g bandwidth, while the Cr t_{2g} bandwidth is not changing, as one may see in Fig. 9.

On the other hand, the shorter Si-O bond distance results in the larger shift of the O $2p$ states to the lower energies than in the case Ge. This should lead to an increase of the crystal-field splitting in TM $3d$ shell going from Ge to Si. The direct center of gravity calculation shows that $t_{2g}-e_g$ crystal-field splitting in $NaCrSi_2O_6$ equals to 1.89 eV, while for $NaCrGe_2O_6$, it is 1.68 eV.

VII. Mn-BASED PYROXENES (d^4)

We were able to find the crystal structure for only one Mn-based pyroxene: $NaMnSi_2O_6$ (mineral namansilite). Having one electron in e_g subshell, Mn ion is Jahn-Teller (JT) active. As a result, the "distribution" of long and short Mn-O bonds in MnO_6 octahedron is different from other pyroxenes.

It is known that because of the anharmonic effects the JT distortion around Mn^{3+} ions typically leads to a local elongation of MnO_6 octahedra.[45] These elongated octahedra may in principle be packed differently, leading both to an antiferrodistortive (for example, as in $LaMnO_3$) and to a ferrodistortive (e.g., Mn_3O_4) ordering.

In the edge-sharing geometry the largest gain in the elastic energy may be achieved, if the longest Me-O bonds in neighboring octahedra are parallel to each other. The explicit expressions for the elastic energies of different distortion modes are summarized in Table I of Ref. 46. Among various possible types of parallel JT distortions in the edge-sharing octahedra, the consecutively "twisting" geometry of pyroxenes selects the only variant: the distortion occurs along the O-Mn-O bond connecting two neighboring octahedra (local z axis). Only in this case, the systems gains the energy for both neighbors. The local crystal field due to the presence of side oxygens forming short Mn-O bond, directed only to the SiO_4 tetrahedra, stabilizes single e_g electron on the $3z^2-r^2$ orbital and therefore works in the same directions.

This conclusion is in full agreement with the crystal-structure studies performed in Ref. 22, where the parallel 180° O-Mn-O bonds along the local z axis connecting neighboring MnO_6 octahedra were found to be the longest.

In the LSDA+U calculations, we indeed obtained that on all of Mn^{3+} ions the single e_g electron localizes on the same $3z^2-r^2$ orbital, directed along this longest Mn-O bond. The resulting magnetic moment equals to $3.69\mu_B$, bang gap of $\sim$1.76 eV. The intrachain exchange calculated in LEIP procedure is AFM and $\sim$3.4 K (from the total energy difference in pseudopotential code, we obtained that $J=-0.1$ K).

The $t_{2g}-t_{2g}$ and $t_{2g}-e_g$ contributions to the total exchange are AFM and equal to 2.1 and 6.1 K, respectively. The situation with half-filled $t_{2g}-t_{2g}$ subshells is the same as in the case of Cr, but $t_{2g}-e_g$ exchange will now predominantly go from the *occupied* t_{2g} to *occupied* e_g orbitals, as shown in Fig. 3(b). This contribution should be AFM, following from Eq. (3). The e_g-e_g contribution is about −4.8 K FM.

VIII. Fe-BASED PYROXENES (d^5)

The Fe^{3+} ions have the simple configuration $d^5(t_{2g}^3e_g^2)$, without any orbital degeneracy; thus, the exchange is uniform along the chain. Using LEIP formalism, we obtained that the intrachain exchange is AFM both in $LiFeSi_2O_6$ ($J=15.8$ K) and $NaFeSi_2O_6$ ($J=15.9$ K). This is consisted with neutron measurement performed in Ref. 5 for $LiFeSi_2O_6$, but disagrees with the experimental findings for $NaFeSi_2O_6$ presented in Ref. 23, where Fe ions were claimed to be ferromagnetically ordered in the chain.

The $t_{2g}-t_{2g}$ partial contribution to the exchange in Fe pyroxenes was found to be AFM and of order of that for Cr-

based ones: 0.5 and 1.4 K for $LiFeSi_2O_6$ and $NaFeSi_2O_6$, respectively. The $t_{2g}-e_g$ exchange is also AFM since it goes from the *occupied* t_{2g} to *occupied* e_g orbitals, as in the case of $NaMnSi_2O_6$. It equals to 9.4 and 7.0 K, respectively.

The situation with e_g-e_g contribution here is a bit different from the case of $NaMnSi_2O_6$. The TM–O–TM angle equals to ~97.1° in $NaMnSi_2O_6$, while in $NaFeSi_2O_6$ and $LiFeSi_2O_6$, it is larger: ~100.5° and ~99.0°, respectively. This may be significant since in deviating from 90°, small FM contribution given by Eq. (5) is quickly outbalanced by much stronger AFM exchange of order t^2/U_{dd}. Detailed analysis shows that the borderline, where the mutual compensation occurs, is about 97°.[47] Thus, one may expect that in Fe-based pyroxenes e_g-e_g exchange will be already AFM. Note, however, that such a strong angle dependence is not a common feature of all the 90° contributions described in Sec. II. For instance, the important for the cromates $t_{2g}-e_g$ exchange is almost angle independent.

Our LEIP calculation confirms this qualitative discussion. The e_g-e_g contribution in Fe pyroxenes is indeed AFM and equals to 5.9 and 7.4 K for $LiFeSi_2O_6$ and $NaFeSi_2O_6$, respectively.

Thus, from a theoretical point of view, it is hard to expect that the intrachain exchange would be FM, as the authors of Ref. 23 proposed. We see that the exchange constants and their partial contributions obtained in LEIP formalism agree with the theoretical conclusions based on the perturbation theory. However, they are obviously too large to describe experimentally observed paramagnetic Curie temperatures: $\Theta=-25.8$ K for $LiFeSi_2O_6$ (Ref. 5) and $\Theta=-46$ K for $NaFeSi_2O_6$.[23]

In contrast to other pyroxenes, the results of total energy calculations in the case of Fe-based pyroxenes differ from those obtained in LEIP formalism. The solution with AFM ordering in the chain was found to have lowest total energy for both Fe-based pyroxenes, and the intrachain exchanges extracted from comparison of AFM and FM total energies are 7 and 8.5 K for $LiFeSi_2O_6$ and $NaFeSi_2O_6$, respectively. The difference with the LEIP results appears because of the strong polarization of oxygen $2p$ shell. This contribution is not explicitly (only via hybridization effects) taken into account in the present LEIP formulation since both the Green functions used in Eq. (8) and defined in Eq. (9), and the potential correction Δ_{ij} are calculated only for transition metal $3d$ states. The values of exchange constants obtained from the total energies agree much better with the experimental values of the Curie temperature.

The detailed explanation of the origin of the difference in the results for the exchange constants obtained by LEIP and from the total energies for Fe pyroxenes is the following. According to the crystal structure of pyroxenes, all the oxygens surrounding every transition metal ion can be divided on two categories. There are two side oxygens linking TMO_6 octahedra and $Si(Ge)O_4$ tetrahedra, and four oxygens connecting neighboring octahedra, as shown in Fig. 2(b). In the case of AFM intrachain coupling, those four oxygens are situated in the compensated field and will not have any polarization. Two other oxygens may be magnetized if the exchange field is large enough. For the FM chains, both types of oxygens will be polarized. Such a polarization will lead to an addition magnetic contribution in the total energy calculation.

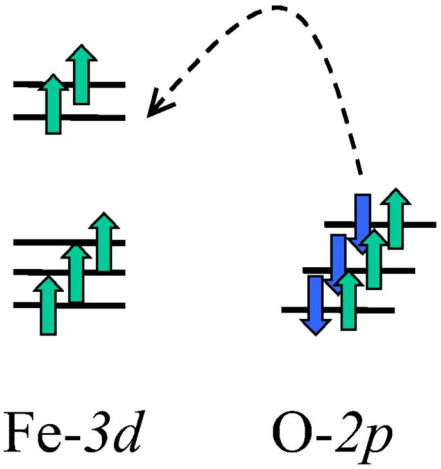

FIG. 10. (Color online) Sketch illustrating mechanism of the spin polarization on oxygen ions in Fe-based pyroxenes.

This effect is especially important and pronounced for the pyroxenes, based on the late transition metal ions. Those ions have large magnetic moment and hence could easier magnetize oxygens. Even more important is the other factor: the nonzero magnetization of oxygen implies strong mixing of magnetic d states of TM with one of O $2p$ orbitals of the same spin, and therefore, it will be much stronger for TM ions with partially filled e_g subshell. For Fe-based pyroxenes with half-filled e_g shell, this effect is rather large: the average magnetic moment on oxygens, lying between TMs, is $0.17\mu_B$ for $LiFeSi_2O_6$ and $0.16\mu_B$ for $NaFeSi_2O_6$. The oxygen moments are directed parallel to those of Fe. It is clearly seen from Fig. 10: only hoppings with antiparallel spin are possible between O $2p$ to Fe $3d$ shells.

Additional polarization of O $2p$ shell in FM solution will lower its total energy. Qualitatively, one may consider it as follows. In the AFM case, both spin up and down electrons would hop from oxygen to different iron ions, while only spin down electrons will be active ones in FM situation, as shown in Fig. 10. Because of Hund's rule coupling on oxygen, the latter (FM solution) will gain more energy.

It is easy to estimate the lowering of the FM total energy because of the oxygen polarization recalling that the gain in magnetic energy in the band theory equals to

$$E_O = -IM^2/4, \tag{10}$$

where I is the Stoner parameter defined as the second derivative of the exchange-correlation energy with respect to the magnetic moment M,

$$I = -2\partial^2 E_{xc}/\partial^2 M. \tag{11}$$

The Stoner exchange constant I for the oxygen $2p$ shell was estimated to be $I=1.6$ eV in Ref. 48 and 49 using constrained LDA calculations.

Recalculating the total energy contribution given by Eq. (10) in terms of the exchange constants for Heisenberg Hamiltonian and taking into account that there are four po-

larized oxygens per two formula (without two side oxygens), we obtained that the exchange corrections due to the oxygen polarization are 10.7 and 9.5 K for $LiFeSi_2O_6$ and $NaFeSi_2O_6$, respectively. The difference between these values and those number obtained in LEIP formalism is a little bit larger than the exchange extracted from the total energy calculations. This seems to be because we did not account for the changes in the one-electron energies (relaxations), which tends to compensate the magnetic corrections given in Eq. (10).

Finally, it is important to note that the contribution, which comes from the polarization effects on oxygen, is not a unique feature of pyroxenes. It was recently found to be crucial for the description of the magnetic interactions in Li_2CuO_4.[49] Authors of Ref. 49 originally interpreted this effect in the manner of initial ideas of Heisenberg as the exchange between Wannier functions (constructed out of TM d and O $2p$ orbitals) due to the Coulomb interaction. It is interesting to note that the final expression for the correction presented in Eq. 22 of Ref. 49 is exactly the same as ours written in Eq. (10), if one uses the substitution $\beta = M(O)/2$.

IX. INTERCHAIN EXCHANGE

In addition to the intrachain exchange interaction, we calculated for Fe-based pyroxenes the interchain ones. It is especially important for the analysis of a possible origin of multiferroicity in Fe-based pyroxenes.[1] The results reflect the general tendency for interchain exchanges in the whole pyroxenes family. There are two types of interchain paths, as depicted in Fig. 2(a): some of TM ions in different chains are connected via two SiO_4 (GeO_4) tetrahedra (J_2), while the others via only one (J_1).

First of all, we found that the interchain exchange is much weaker than the intrachain one. Then, we found that for both $LiFeSi_2O_6$ and $NaFeSi_2O_6$, J_2 is, indeed, approximately two times larger than J_1: $J_1^{Li}=1.9$ K, $J_2^{Li}=3.4$ K, $J_1^{Na}=0.8$ K, and $J_2^{Na}=1.6$ K. In addition, one may see that the change of Li ions to Na leads to a significant decrease of interchain exchange interaction. It is connected with larger ionic radii of Na (in sixfold coordination $R_{Li^+}=0.76$ Å, while $R_{Na^+}=1.02$ Å).

X. CONCLUSIONS

In this paper, using *ab initio* LSDA+U calculations, we carried out the detailed analysis of electronic structure and especially of the exchange interaction in a broad class of quasi-one-dimensional magnetic systems—pyroxenes containing transition metal ions. We analyzed the systematics of the exchange interactions and compared it with the simple rules following from the perturbation theory.

The exchange interaction due to direct hopping between t_{2g} orbitals (which we call "direct exchange interaction") dominates in early transition (Ti,V) metal-based pyroxenes. In $NaTiSi_2O_6$ single d electron localizes on the zy orbital, which results in a strong AFM coupling in one out of two Ti-Ti pairs. This leads to the dimerization of TiO_6 chains and the formation of a spin gap on singlet Ti-Ti dimers.

The nonuniformity of the exchange interaction disappears in d^2 pyroxenes, such as $(Li,Na)VSi_2O_6$, where electrons occupy zx and zy orbitals. This type of orbital filling is determined by a common structural feature of all pyroxenes (except Jahn-Teller ones): the presence of two short TM–O bonds perpendicular to a local z axis (directed along single 180° O–TM–O bond connecting two neighboring TMO_6 octahedra).

With an increase of the number of d electron, the AFM $t_{2g}-t_{2g}$ direct exchange interaction is gradually suppressed due to an increase of the on-site Coulomb interaction (U), and the $t_{2g}-t_{2g}/e_g$ superexchange contributions (most of which are FM) starts to play a more important role, especially because of the decrease of the charge-transfer energy, which enters the corresponding expressions for the exchange in Eqs. (2)–(5) in the denominator. In Cr-based pyroxenes (d^3), the AFM $t_{2g}-t_{2g}$ exchange interaction is nearly compensated by the FM $t_{2g}-e_g$ exchange. The crystal structure makes a fine tuning of these contributions, and $NaCrGe_2O_6$ with largest Cr-Cr distance turns out to be FM.

In $NaMnSi_2O_6$, Mn^{3+} is a Jahn-Teller ion. We show that the consecutive "twisting" geometry of pyroxenes and the tendency to gain an elastic energy result in the ferro type of distortion with the local z axis becoming the longest one.

Iron-based pyroxenes were found to be AFM, with the large oxygen polarization ($\mu_O \sim 0.2\mu_B$). This effect is usually ignored in the literature.[13] However, we show that it considerably reduces (by $\sim 2/3$) the AFM superexchange interaction. The total energy of the FM state is lowered because of the gain in Hund's rule coupling in O $2p$ shell, which turns out be polarized in this state. The interchain exchange coupling was estimated for Fe-based pyroxenes and found to be small and AFM.

The presented results give a rather complete description of exchange interactions in magnetic pyroxenes, and it may serve as a basis for the further study of magnetism and other properties, including multiferroicity, of this interesting class of materials.

ACKNOWLEDGMENTS

We are grateful to G. Redhammer, who took up our call to measure the crystal structure of $NaCrGe_2O_6$, to N. Binggeli for the help with pseudopotential code, and to V. Anisimov and V. Mazurenko for their invaluable help in interpretations of magnetic calculations for Fe-based pyroxenes. This work is supported by UrD RAS, Dynasty Foundation and International Center for Fundamental Physics in Moscow, by INTAS Foundation via YS grant No. 05-109-4727, by the Russian Ministry of Science and Education together with the Civil research and development foundation through Grant No. Y4-P-05-15, by the Russian president grant for young scientists MK-1184.2007.2, by the Russian Foundation for Basic Research through RFFI-07-02-00041 and 06-02-81017, and by SFB 608.

*streltsov@optics.imp.uran.ru

[1] S. Jodlauk, P. Becker, J. A. Mydosh, D. I. Khomskii, T. Lorenz, S. V. Streltsov, D. C. Hezel, and L. Bohaty, J. Phys.: Condens. Matter **19**, 432201 (2007).

[2] S.-W. Cheong and M. Mostovoy, Nat. Mater. **6**, 13 (2007).

[3] D. I. Khomskii, J. Magn. Magn. Mater. **306**, 1 (2006).

[4] A. N. Vasiliev, O. L. Ignatchik, M. Isobe, and Y. Ueda, Phys. Rev. B **70**, 132415 (2004).

[5] G. J. Redhammer, G. Roth, W. Paulus, G. Andre, W. Lottermoser, G. Amthauer, W. Treutmann, and B. Koppelhuber-Bitschnau, Phys. Chem. Miner. **28**, 337 (2001).

[6] A. N. Vasiliev, O. L. Ignatchik, A. N. Sokolov, Z. Hiroi, M. Isobe, and Y. Ueda, Phys. Rev. B **72**, 012412 (2005).

[7] Y. Sasago, M. Hase, K. Uchinokura, M. Tokunaga, and N. Miura, Phys. Rev. B **52**, 3533 (1995).

[8] M. Isobe, E. Ninomiya, A. N. Vasilev, and Y. Ueda, J. Phys. Soc. Jpn. **71**, 1423 (2002).

[9] S. V. Streltsov, O. A. Popova, and D. I. Khomskii, Phys. Rev. Lett. **96**, 249701 (2006).

[10] R. Valenti, T. Saha-Dasgupta, and Claudius Gros, Phys. Rev. B **66**, 054426 (2002).

[11] J. van Wezel and J. van den Brink, Europhys. Lett. **75**, 957 (2006).

[12] One should not mix our direct exchange with the standard Heisenberg exchange. The first one is caused by virtual hoppings of d electrons to neighboring sites $J \propto 2t_{ij}^2/U_{dd}$, and is not due to an exchange part of the Coulomb interaction $J_{ij}^{Heis} = \int \phi_i^*(r)\phi_j(r)\phi_j^*(r')\phi_i(r')/(|r-r'|)drdr'$, as the second one.

[13] J. B. Goodenough, *Magnetism and the Chemical Bond* (Interscience, New York, 1963).

[14] W. A. Harrison, *Elementary Electronic Structure* (World Scientific, Singapore, 1999).

[15] A. E. Bocquet, T. Mizokawa, K. Morikawa, A. Fujimori, S. R. Barman, K. Maiti, D. D. Sarma, Y. Tokura, and M. Onoda, Phys. Rev. B **53**, 1161 (1996).

[16] G. J. Redhammer, H. Ohashi, and G. Roth, Acta Crystallogr., Sect. B: Struct. Sci. **59**, 730 (2003).

[17] C. Satto, P. Millet, and J. Galy, Acta Crystallogr., Sect. C: Cryst. Struct. Commun. **53**, 1727 (1997).

[18] H. Ohashi, T. Osawa, and A. Sato, Acta Crystallogr., Sect. C: Cryst. Struct. Commun. **50**, 1652 (1994).

[19] G. J. Redhammer and G. Roth, Z. Kristallogr. **219**, 585 (2004).

[20] M. Origlieri, R. T. Downs, R. M. Thompson, C. J. S. Pommier, M. B. Denton, and G. E. Harlow, Am. Mineral. **88**, 1025 (2003). Please note that the coordinates given in the paper contain an error. The y coordinate of O2 was corrected to be 0.25893 in order to correspond to the distance calculations.

[21] G. J. Redhammer (private communication).

[22] H. Ohashi, T. Osawa, and K. Tsukimura, Acta Crystallogr., Sect. C: Cryst. Struct. Commun. **43**, 605 (1987).

[23] O. Ballet, J. M. D. Coey, G. Fillion, A. Ghose, A. Hewat, and J. R. Regnard, Phys. Chem. Miner. **16**, 672 (1989).

[24] M. Emirdag-Eanes and J. W. Kolis, Mater. Res. Bull. **39**, 1557 (2004).

[25] B. Pedrini, J. L. Gavilano, D. Rau, H. R. Ott, S. M. Kazakov, J. Karpinski, and S. Wessel, Phys. Rev. B **70**, 024421 (2004).

[26] S. V. Streltsov, A. S. Mylnikova, A. O. Shorikov, Z. V. Pchelkina, D. I. Khomskii, and V. I. Anisimov, Phys. Rev. B **71**, 245114 (2005).

[27] O. K. Andersen and O. Jepsen, Phys. Rev. Lett. **53**, 2571 (1984).

[28] M. I. Katsnelson and A. I. Lichtenstein, Phys. Rev. B **61**, 8906 (2000).

[29] S. Baroni, A. Dal Corso, S. de Gironcoli, P. Giannozzi, C. Cavazzoni, G. Ballabio, S. Scandolo, G. Chiarotti, P. Focher, A. Pasquarello, K. Laasonen, A. Trave, R. Car, N. Marzari, and A. Kokali, plane-wave self-consistent field PWSCF codes (http://www.pwscf.org/).

[30] V. I. Anisimov, D. E. Kondakov, A. V. Kozhevnikov, I. A. Nekrasov, Z. V. Pchelkina, J. W. Allen, S.-K. Mo, H.-D. Kim, P. Metcalf, S. Suga, A. Sekiyama, G. Keller, I. Leonov, X. Ren, and D. Vollhardt, Phys. Rev. B **71**, 125119 (2005).

[31] P. J. Baker, S. J. Blundell, F. L. Pratt, T. Lancaster, M. L. Brooks, W. Hayes, M. Isobe, Y. Ueda, M. Hoinkis, M. Sing, M. Klemm, S. Horn, and R. Claessen, Phys. Rev. B **75**, 094404 (2007).

[32] M. J. Konstantinović, J. van den Brink, Z. V. Popović, V. V. Moshchalkov, M. Isobe, and Y. Ueda, Phys. Rev. B **69**, 020409(R) (2004).

[33] F. D. M. Haldane, Phys. Rev. Lett. **50**, 1153 (1983).

[34] Z. S. Popović, Z. V. Šlijivančanin, and F. R. Vukajlović, Phys. Rev. Lett. **93**, 036401 (2004).

[35] Z. S. Popović, Z. V. Šljivančanin, and F. R. Vukajlović, Phys. Rev. Lett. **96**, 249702 (2006).

[36] G. L. Gutsev and C. W. Bauschlicher, Jr., J. Phys. Chem. A **107**, 4755 (2003).

[37] K. I. Kugel and D. I. Khomskii, Usp. Fiz. Nauk **136**, 621 (1982).

[38] J. L. Gavilano, S. Mushkolaj, H. R. Ott, P. Millet, and F. Mila, Phys. Rev. Lett. **85**, 409 (2000) , Eur. Phys. J. B **55**, 219 (2007).

[39] P. Millet, F. Mila, F. C. Zhang, M. Mambrini, A. B. Van Oosten, V. A. Pashchenko, A. Sulpice, and A. Stepanov, Phys. Rev. Lett. **83**, 4176 (1999).

[40] B. Pedrini, J. L. Gavilano, H. R. Ott, S. M. Kazakov, J. Karpinski, and S. Wessel, Eur. Phys. J. B **55**, 219 (2007).

[41] M. D. Lumsden, G. E. Granroth, D. Mandrus, S. E. Nagler, J. R. Thompson, J. P. Castellan, and B. D. Gaulin, Phys. Rev. B **62**, R9244 (2000).

[42] M. A. Korotin, V. I. Anisimov, D. I. Khomskii, and G. A. Sawatzky, Phys. Rev. Lett. **80**, 4305 (1998).

[43] Quite similar behavior was found in $CrCrO_3$. S. V. Streltsov, M. A. Korotin, V. I. Anisimov, and D. I. Khomskii (unpublished).

[44] It is hard to estimate explicitly a precision of the band structure calculation for the exchange constants computations since it depends on many implicit factors such as type of the approximation, etc. We tried to change some internal parameters of our calculation scheme as R_{MT}, linearization energies, and so on and estimate it to be 2–3 K for $S=3/2$.

[45] D. I. Khomskii and J. van den Brink, Phys. Rev. Lett. **85**, 3329 (2000).

[46] D. I. Khomskii and K. I. Kugel, Phys. Rev. B **67**, 134401 (2003).

[47] W. Geertsma and D. I. Khomskii, Phys. Rev. B **54**, 3011 (1996).

[48] I. I. Mazin and D. J. Singh, Phys. Rev. B **56**, 2556 (1997).

[49] V. V. Mazurenko, S. L. Skornyakov, A. V. Kozhevnikov, F. Mila, and V. I. Anisimov, Phys. Rev. B **75**, 224408 (2007).